THE JOURNAL OF BIOLOGICAL CHEMISTRY VOL. 283, NO. 18, pp. 12586–12594, May 2, 2008
© 2008 by The American Society for Biochemistry and Molecular Biology, Inc. Printed in the U.S.A.

A Distinctive Physiological Role for IκBβ in the Propagation of Mitochondrial Respiratory Stress Signaling*

Received for publication, December 24, 2007 Published, JBC Papers in Press, February 13, 2008, DOI 10.1074/jbc.M710481200

Gopa Biswas‡, Weigang Tang‡, Neal Sondheimer§, Manti Guha‡, Seema Bansal‡, and Narayan G. Avadhani‡1

From the ‡Department of Animal Biology and Mari Lowe Center for Comparative Oncology, School of Veterinary Medicine, University of Pennsylvania, Philadelphia, Pennsylvania 19104 and §Section of Biochemical Genetics, The Children's Hospital of Philadelphia, Philadelphia, Pennsylvania 19104

The NFκBs regulate an array of physiological and pathological processes, including propagation of mitochondrial respiratory stress signaling in mammalian cells. We showed previously that mitochondrial stress activates NFκB using a novel calcineurin-requiring pathway that is different from canonical or non-canonical pathways. This study shows that IκBβ is essential for the propagation of mitochondrial stress signaling. Knock down of IκBβ, but not IκBα, mRNA reduced the mitochondrial stress-mediated activation and nuclear translocation of cRel:p50, inhibiting expression of nuclear target genes RyR1 and cathepsin L. IκBβ mRNA knock down also reduced resistance to staurosporine-induced apoptosis and decreased *in vitro* invasiveness. Induced receptor switching to insulin-like growth factor-1 receptor and increased glucose uptake are hallmarks of mitochondrial stress. IκBβ mRNA knock down selectively abrogated the receptor switch and altered tubulin cytoskeletal organization. These results show that mitochondrial stress signaling uses an IκBβ-initiated NFκB pathway that is distinct from the other known NFκB pathways. Furthermore, our results demonstrate the distinctive physiological roles of the two inhibitory proteins IκBβ and IκBα.

NFκB transcription factors play critical roles in the regulation of genes associated with T-cell differentiation, immunity, inflammatory response, cell proliferation/transformation, apoptosis, and metastasis. The NFκB pathway responds to a battery of extracellular and intracellular stimuli (for a comprehensive review see Ref. 1), and the downstream transcriptional activators can be classified into two main groups. The first consists of RelA, RelB, and cRel, all of which contain an N-terminal Rel homology domain that has important roles in protein dimerization and DNA binding. The second group consists of p52 and p50, which are processed from the larger p100 and p105, respectively, by partial ubiquitin-mediated degradation. Two major pathways have been described for the activation of NFκB, namely the canonical and non-canonical pathways. The canonical pathway involves the activation of RelA, cRel, p50 heterodimers that are held in the cytosol by inhibitory IκB proteins, including IκBα, IκBβ, and IκBϵ (2, 3). The physiological functions of different inhibitors and their specificity for various Rel proteins remain unclear. The non-canonical pathway is initiated by the IKKα-mediated phosphorylation of p100, which provides the signal for ubiquitination of p100 and generation of the active p52:RelB dimer (2–6).

The canonical NFκB pathway is stimulated by interleukins, interferons, or chemokines and mediated through phosphorylation and degradation of inhibitory proteins, particularly IκBα. In response to stimulation, IκBα undergoes IKKβ-dependent phosphorylation and ubiquitin-mediated degradation, liberating the NFκB heterodimer. The active heterodimer with unmasked nuclear localization signal is then translocated to the nucleus to carry out its transcriptional activity (2–6). Many studies of the canonical pathway have focused on IκBα and its interaction with heterodimeric RelA/p50 proteins. It has been generally assumed that the same mechanism of regulation by inhibitor degradation applies to IκBβ.

The many implied roles of the NFκB pathway and its response to diverse stimuli (3, 7, 8) suggest additional mechanisms of activation of this pathway. For example, an IKK-independent pathway involving CKII or tyrosine kinase-mediated phosphorylation of IκBα at sites other than the IKK target sites has been reported. The precise physiological roles of different pathways and their selectivity for different Rel proteins remain unclear (9–13). Most of the NFκB dimers activate common target genes that coordinate inflammatory response, immune regulation, cell cycle, cell survival, and tumorigenesis.

A number of studies, including ours, have shown that mitochondrial respiratory stress induced by multiple causes, including mitochondrial respiratory inhibitors, partial or complete mtDNA depletion (14–19), mtDNA mutations (20, 21), suppression of mitochondrial transcription (22), and hypoxia (23), induce a mitochondrial stress signaling pathway that is analogous to the retrograde signaling pathway described in yeast cells (24). In contrast to the multifunctional Rtg factors in yeast cells (25–29), the mitochondrial stress signaling in mammalian cells occurs through increased cytosolic $[Ca^{2+}]_c$ and activation of cytosolic protein phosphatase calcineurin (Cn).[2] Recently, the

* This work was supported by National Institutes of Health Grant CA-22762. The costs of publication of this article were defrayed in part by the payment of page charges. This article must therefore be hereby marked "*advertisement*" in accordance with 18 U.S.C. Section 1734 solely to indicate this fact.

[1] To whom correspondence should be addressed: Dept. of Animal Biology, School of Veterinary Medicine, University of Pennsylvania, 3800 Spruce St., Philadelphia, PA 19104. Tel.: 215-898-8819; Fax: 215-573-6651; E-mail: narayan@vet.upenn.edu.

[2] The abbreviations used are: Cn, calcineurin; ΔΨm, mitochondrial membrane potential; RyR1, ryanodine receptor 1; CathL, cathepsin L; IGF-1R, insulin-like growth factor-1 receptor; Glut4, glucose transporter 4; CCCP; carbonyl cyanide-m chlorophenylhydrazone; TNF, tumor necrosis factor; IL-6, interleukin 6; KD, knock down; MnSOD, manganese superoxide dismutase; siRNA, small interfering RNA; STP, staurosporine.

mitochondrial dysfunction and associated respiratory stress signaling have been proposed to play a role in aging and age-related pathologies (24).

Activation of Cn, which is a critical upstream effecter of the mitochondrial respiratory stress pathway (14, 27, 28), causes preferential activation and nuclear localization of cRel:p50 dimers and also a number of other Ca^{2+}-responsive factors (28–30). Knock out of Calcineurin Aα (CnAα) or inhibition of Cn activity by FK506 increased the levels of phosphorylated IκBβ in the cytoplasm and reduced nuclear levels of cRel and p50. We showed that the binding of Cn to the IκBβ-cRel:p50 complex and subsequent dephosphorylation of IκBβ causes the release and nuclear translocation of active cRel:p50 heterodimer. This pathway is independent of IKK but likely involves CKII-dependent phosphorylation of IκBβ at Ser-313 and Ser-315 of the C-terminal PEST II domain. Dephosphorylation of IκBβ at these sites in the PEST II domain by Cn is a critical and necessary step for the mitochondrial stress-mediated activation of cRel:p50 heterodimer, and mutations S313A and S315A of IκBβ severely curtailed NFκB activation through this pathway (28). In conjunction with other transcription factors that are activated as part of the mitochondrial respiratory stress pathway, cRel:p50 heterodimers activate an array of target genes involved in Ca^{2+} regulation, glucose metabolism and, most importantly, tumor promotion (15, 16, 27–31). These targets are not considered classical NFκB-responsive genes. Studies by our and other laboratories show that mitochondrial respiratory stress signaling induces a metabolic shift through activation of IGF-1R-phosphatidylinositol 3-kinase pathway and also AKT. Inhibition of IGF-1R and phosphatidylinositol 3-kinase induced apoptosis in cells subjected to mitochondrial stress (31–34).

In this report, we have elucidated the unique and distinctive role of IκBβ in the propagation of mitochondrial respiratory stress signaling, activation of several marker genes, and development of stress-induced invasive phenotypes. Our results show that many of these characteristics of mtDNA-depleted cells are reversed by knock down of IκBβ. Although it is generally believed that the roles of IκBα and IκBβ in NFκB signaling are indistinguishable, the present study shows that IκBβ and IκBα have distinct physiological roles in responding to mitochondrial respiratory stress.

MATERIALS AND METHODS

Cell Lines and Culture Conditions—Murine C2C12 skeletal myoblasts (ATCC CRL1772) were grown in Dulbecco's modified Eagle's medium (Invitrogen) supplemented with 10% fetal bovine serum and 0.1% gentamycin as described before (14). Partial depletion of mtDNA was carried out by treatment with ethidium bromide (100 ng/ml) as described before (14). Selected clones containing ~15% mtDNA contents were grown in the presence of 1 mM sodium pyruvate and 50 μg/ml uridine. Reverted cells represent mtDNA-depleted cells (with ~15% mtDNA contents) grown for 30 cycles in the absence of ethidium bromide until the mtDNA content was reverted back to ~80% of control cells. The mtDNA contents were monitored either by real-time PCR or Southern blot hybridization as described before (14, 27).

Stable Expression of siRNA and Knock Down of IκBβ and IκBα mRNAs—Two siRNA sequences targeting mouse IκBβ (5′-GACTGGAGGCTACAACTAG-3′ and 5′-CAGAGATGAGGGCGATGAA-3′) were designed and cloned into pSilencer 1.0-U6 vector (Ambion). Empty pSilencer 1.0-U6 vector was used as control. Control and siRNA vector were co-transfected with neomycin-resistant pcDNA3 vector (Invitrogen) into control and depleted cells. G418 (1 mg/ml) was added to the medium for selection. Two siRNA sequences against mouse IκBα (5′-AGGCCAGCGTCTGACATTA3-′ and 5′-GGCCAGCGTCTGACATTAT-3′) were cloned in pSUPER retro puro vector (OligoEngine). 293T cells were infected with the retroviral clones and the vector alone. The medium was used to infect control and mtDNA-depleted cells in the presence of 6 μg/ml polybrene. Selection was done in the presence of puromycin (10 μg/ml) for control cells and 100 μg/ml for depleted cells because these cells were resistant to lower dose of the antibiotic. After 3 weeks, well separated individual colonies were picked and grown. The protein levels of IκBβ and IκBα were checked by Western blot using antibodies against respective protein (Santa Cruz Biotechnology). Cells with significantly lower level of IκBβ or IκBα compared with their respective controls were taken as stable knockdown cells for further study.

Subcellular Fractionation and Immunoblot Analysis—The subcellular fractions were prepared essentially as described before (14, 28) in the presence of protease and phosphatase inhibitors. Proteins (30 μg each) were resolved on 10 or 12% SDS-polyacrylamide gels and detected by Western blot analysis as described as before (14). Blots were developed using Super Signal West Femto maximum sensitivity substrate (Pierce).

Measurement of Mitochondrial Membrane Potential—The mitochondrial membrane potential (ΔΨm) was assayed spectrofluorometrically by loading the cells with a cationic dye, Mito Tracker Orange CM-H_2 TMRos (MTO) (Molecular Probe Inc.) as described before (15). The rate of dye uptake was recorded as a measure of ΔΨm using a Delta RAM PTI spectrofluorometer at 525 ex/575 em as fluorescence units/min.

Calcium Release Assay—Ca^{2+} release was measured essentially as described before (15, 35). The cells were suspended in intracellular medium (20 mM HEPES-Tris, pH 7.2, 120 mM NaCl, 5 mM KCl, 1 mM KH_2PO_4) passed through a Chelex (Sigma) column to remove residual Ca^{2+}. The cells were loaded with membrane-permeable Fura 2FF/FA (1 μM) for 20 min at room temperature, pelleted, and resuspended in 1 ml of intracellular medium for measuring both basal [Ca^{2+}] as well as the RyR1-specific Ca^{2+} release in response to 20 mM caffeine and 10 μM acetylcholine. Fluorescence was monitored at excitation 340/380 nm and emission 510 nm. Calibration of Fura 2FF/FA signal was carried out using a calibration buffer (10 mM EGTA-Tris-HEPES, pH 8.5, and 5 mM $CaCl_2$).

Microarray Analysis—Total RNA from control, mtDNA-depleted, IκBβ knock down (KD)/Control, and IκBβ KD/Depleted C2C12 cells was isolated using TRIzol according to the manufacturer's instructions. RNA was analyzed on MOE430A chips (Affymetrix). Statistical significance established with Partek (two-way analysis of variance significant to <0.0005). Gene selection was performed using the Spotfire program. The total number of spots matching criteria was 43, representing 25 Gene Ontology header-mapped genes with known functions.

Real-time PCR—Total RNA (5 μg) from cells was reverse-transcribed using the High Capacity cDNA Archives kit (Applied Biosystems, Inc.). Real-time amplifications were performed using specific primers in an ABI 7300 real-time PCR machine using SYBR Green Master Mix (ABI). Each 25-μl reaction contained 25 ng of cDNA and 200 nM forward and reverse primers. Two-step reverse transcription PCR was carried for 40 cycles. Data were analyzed using ABI Relative Quantitation analysis software. β-Actin served as an internal control. Target gene expression was presented as -fold increase over control levels.

Glucose Uptake Assay—Glucose uptake using 2-[^{3}H]deoxyglucose was measured as described before (31, 36). 1×10^6 cells grown in 6-well plates were serum-starved for 4 h and incubated for 30 min in glucose-free medium. 1 μCi of 2-[^{3}H]deoxyglucose was added and incubated for 15 min. Cells were rapidly chilled to 4 °C, washed four times at 4 °C, and transferred to scintillation vials for counting.

Matrigel Invasion Assay—The *in vitro* invasion assays were carried out as described previously (16). 4×10^4 cells were layered into the invasion chambers containing 1:3 diluted Matrigel (BD Biosciences) and incubated in wells (12-well plates) containing 1 ml of growth medium in each well for 24–48 h at 37 °C. Matrigel layers with non-invading cells were removed, and the membranes with invaded cells were stained with Meyer's hematoxylin, cut, and mounted on slides to view under the bright field Olympus BX61 microscope.

Adherence-independent Growth Assay on Soft Agar—The cells (2×10^3/well) were suspended in soft agar (2%) mixed with growth medium and plated in 12-well plates. After 48 h of incubation the plates were imaged and photographed using a bright field imaging microscope.

Immunocytochemistry—Cells were grown on coverslips and processed for antibody staining essentially as described before (14, 28). Cells were immunostained with 1:100 dilution of primary antibody for 1 h and 1:100 dilutions of Alexa Fluor-conjugated secondary antibody for 1 h at 37 °C. Fluorescence microscopy was carried out using an Olympus BX61 fluorescence microscope.

RESULTS

Distinct Roles of IκBβ and IκBα in the Mitochondrial Respiratory Stress-mediated Activation of NFκB—To establish the roles of inhibitory IκB proteins in the propagation of mitochondrial respiratory stress signaling, we generated cell lines deficient in IκBα or IκBβ by siRNA expression (named IκBα KD and IκBβ KD, respectively) from control and depleted C2C12 murine skeletal myoblasts (14). As shown in Fig. 1*A*, IκBα and IκBβ knock down (KD) by mRNA silencing in control and mtDNA-depleted cells (hereafter called depleted cells) markedly diminished the levels of these respective proteins without affecting the levels of the other protein. Silencing the IκBβ mRNA in mtDNA-depleted cells (hereafter called IκBβ KD/Depl) caused reduced nuclear levels of cRel and p50 proteins when compared with mtDNA-depleted cells with mock transfection (Fig. 1*B*). On the other hand, cRel and p50 levels in the cytoplasm were increased by IκBβ silencing in depleted cells as compared with control cells although the level of cytoplasmic CnAα remained the same in IκBβ KD/Depl cells as

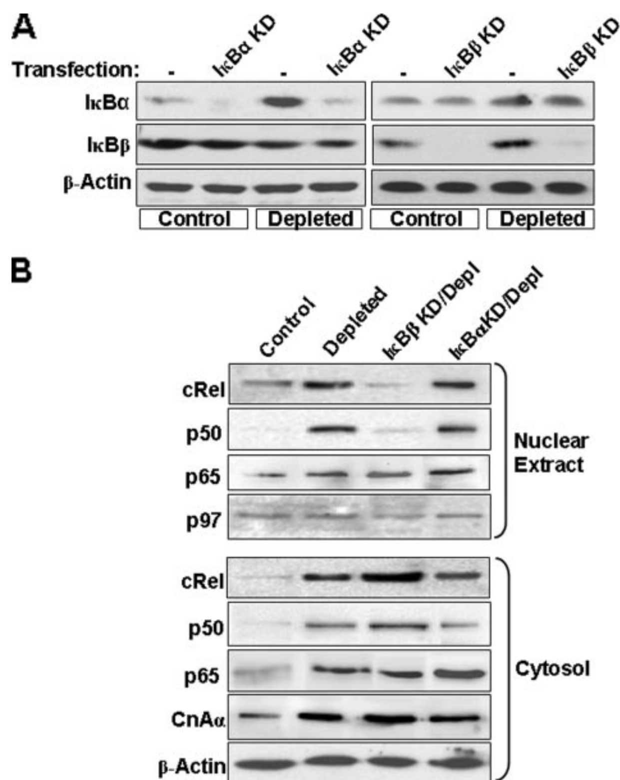

FIGURE 1. **Distinctive effects of knock down of IκBα and IκBβ mRNAs in control C2C12 and mtDNA-depleted cell lines.** *A*, cell lines stably expressing siRNAs targeted for IκBα or IκBβ mRNAs were generated as described under "Materials and Methods." The IκBα (*top row*) and IκBβ (*middle row*) protein levels in IκBα knockdown (IκBα KD, *left panel*) and IκBβ knockdown (IκBβ KD, *right panel*) were determined using the cytosolic fractions of cell lines by immunoblot analysis (50 μg of protein each). Levels of β-actin were used as loading controls (*bottom row*). *B*, levels of mitochondrial-responsive proteins cRel, p50, and calcineurin Aα (*CnAα*) in the nuclear and cytosolic fractions of IκBα KD or IκBβ KD cells. The fractions were isolated and subjected to immunoblot analysis (30 μg each) with indicated antibodies. Levels of p97 and β-actin were used as loading controls for nuclear and cytosolic fractions, respectively.

compared with the depleted cells alone. Knock down of IκBα in depleted cells (hereafter called IκBα KD/Depl), by contrast, did not affect the nuclear or cytoplasmic levels of cRel, p50, or CnAα (Fig. 1*B*). Level of p65 in the nucleus was not significantly affected by knock down of IκBβ but marginally increased by IκBα mRNA knock down. We also observed an increase in levels of cytosolic p65 in these samples. These results show that IκBβ may be selectively involved in responding to mitochondrial respiratory stress.

Temporal Order of Mitochondrial Respiratory Dysfunction, Changes in Ca^{2+} Homeostasis, and Calcineurin-dependent NFκB Activation—To understand the sequence of events leading to NFκB activation, we studied mitochondrial membrane potential (ΔΨm) and cellular Ca^{2+} levels in IκBβ KD/Depl and IκBα KD/Depl cells. Mitochondrial ΔΨm was measured as the rate of uptake of Mitotracker Orange CM-H_2 TMROS in control cells and depleted cells as well as IκBβ KD/Depl and IκBα/Depl cells. The reduced form of the dye is taken up by mitochondria in proportion to ΔΨm, which fluoresces upon oxidation inside respiring mitochondria. Control cell mitochondria exhibited a steeper membrane potential as indicated by a time-dependent increase in fluorescence (Fig. 2*A*). Depleted cells, and also cells

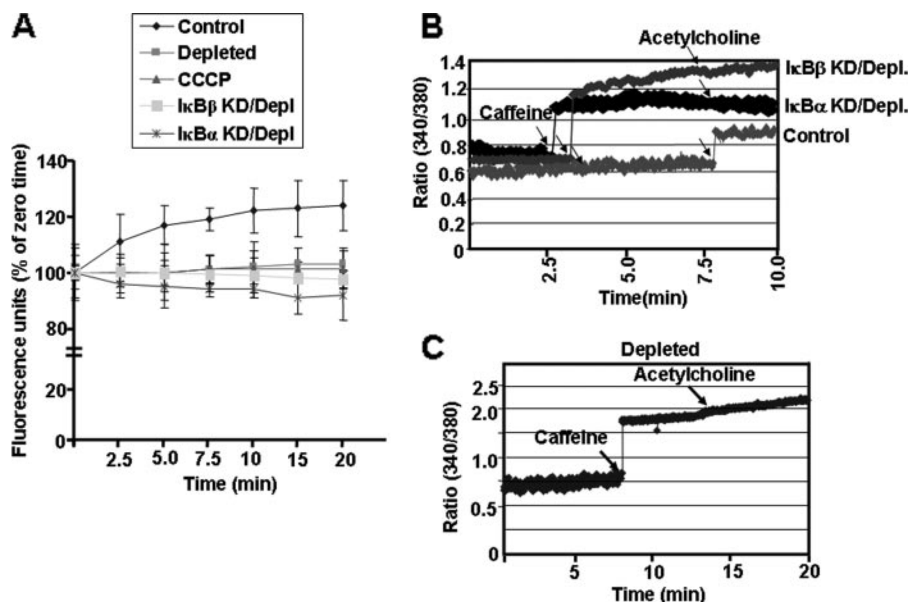

FIGURE 2. **Effects of IκBα or IκBβ mRNA knock down in C2C12 cells on mitochondrial transmembrane potential and Ca^{2+} homeostasis.** *A*, mitochondrial membrane potential was measured in control, mtDNA-depleted (*Depleted*), and IκBβ or IκBα knockdown/depleted cell lines (labeled as *IκBβ KD/Depl* and *IκBα KD/Depl*, respectively) or control cells treated with CCCP as a measure of uptake of Mitotracker Orange dye over a period of 20 min. Each time point represents the average of five readings. *B* and *C*, cytosolic free Ca^{2+} was measured in the indicated cell lines, loaded with Fura 2FF/FA (1 μM). Ca^{2+} release was measured in response to either caffeine (20 mM) or acetylcholine (2 μM) as described under "Materials and Methods."

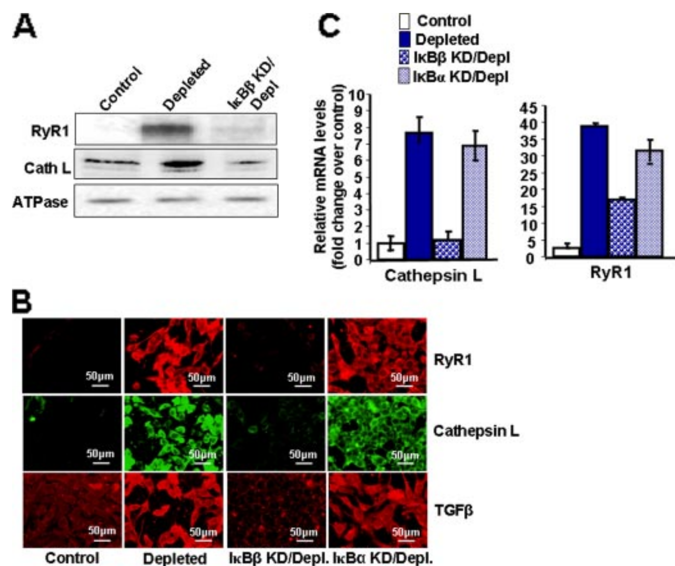

FIGURE 3. **Effects of IκBα or IκBβ mRNA knock down in mtDNA-depleted cells on the levels of expression of respiratory stress-responsive genes.** *A*, steady state levels of Cathepsin L (*Cath L*) and ryanodine receptor 1 (*RyR1*) proteins were detected in total homogenates (30 μg) of control, mtDNA-depleted, and IκBβ KD/Depl cells by immunoblot analysis. Na^{+}/K^{+} ATPase (*ATPase*) was used as loading control. *B*, levels of RyR1, CathL, and transforming growth factor β (*TGFβ*) proteins were determined by immunofluorescent labeling of the indicated cell lines. The cells were grown on coverslips and labeled with the indicated antibodies as described under "Materials and Methods." *C*, mRNA levels of target genes cathepsin L and RyR1 were measured by real-time PCR of total RNA isolated from the indicated cells lines as described under "Materials and Methods." Values represent average of triplicates and were normalized against β-actin as an internal control also run in triplicates.

treated with the mitochondrial ionophore, carbonyl cyanide-m chlorophenylhydrazone (CCCP), showed decreased fluorescence indicative of disrupted ΔΨm. IκBβ and IκBα mRNA knock down had no effect on ΔΨm in depleted cells. Additionally, IκBβ and IκBα mRNA knock down in control cells also did not affect the rate of increase in fluorescence (data not shown). These results suggest that perturbation of ΔΨm is an upstream event that marks the initiation of respiratory stress.

We also assessed steady state Ca^{2+} levels and caffeine-evoked Ca^{2+} release in control, IκBβ KD/Depl, and IκBα KD/Depl cells (Fig. 2*B*). Both IκBα KD/Depl and IκBβ KD/Depl cells had a significant degree of Ca^{2+} release in response to caffeine. These calcium pools represent the RyR1 channel-specific Ca^{2+} stores and are comparable with the responses observed in depleted cells as depicted in Fig. 2*C* (14). Both cell lines also displayed increased basal Ca^{2+} compared with control cells, which is another characteristic feature of depleted cells. In confirmation of our previous results (14), control cells responded only to acetylcholine, an agonist of the inositol triphosphate channel, and did not respond to caffeine. Therefore, this suggests that the marked change in the Ca^{2+} homeostasis and/or steady state levels of Ca^{2+} in response to mitochondrial stress are upstream events from the activity of IκBβ in mitochondrial stress signaling.

Role of IκBβ in the Propagation of Mitochondrial Stress Signaling and Expression of Nuclear Target Genes—In our previous study we showed that mitochondrial stress-mediated activation of NFκB leads to transcriptional activation of a set of genes that are not regarded as classical NFκB targets (28). Fig. 3, *A* and *B*, shows immunoblots of proteins from post-mitochondrial supernatant fraction and immunohistograms of control and mtDNA-depleted C2C12 cells as well as IκBβ KD/Depl and IκBα KD/Depl cells. The levels of RyR1 and cathepsin L (Cath L) were markedly reduced in IκBβ KD/Depl cells as compared with the parent mtDNA-depleted cells (Fig. 3*A*). The effect of IκBβ and IκBα mRNA knock down on the levels of RyR1, Cath L, and transforming growth factor β, another target gene of the stress-signaling pathway, was further validated by immunohistochemical staining. As seen from Fig. 3*B*, knock down of IκBα mRNA did not have a significant effect on the levels of these proteins as judged by the intensity of immunostaining. Expression of RyR1 and Cath L was further measured in terms of mRNA levels using real-time PCR. In line with the immunohistochemical data, results of real-time PCR (Fig. 3*C*) also show that the steady state levels of Cath L and RyR1 mRNAs were significantly reduced in IκBβ KD/Depl cells as compared with the parent depleted cells. IκBα KD/Depl cells had only a marginal effect on the levels of Cath L and RyR1 mRNAs.

To assess the distinctive functional attributes of the two inhibitory proteins, we measured the TNFα-induced expres-

sion of the classical NFκB targets IL-6, MnSOD, and TNFα. IL-6 mRNA was induced 2.5-fold in response to TNFα treatment in mtDNA-depleted cells, while the extent of induction was severely curtailed in IκBα KD/Depl cells (Fig. 4*A*). IκBβ mRNA knock down had no effect upon the extent of TNFα-mediated IL-6 mRNA induction. Surprisingly, IκBβ mRNA knock down caused a nearly 9-fold induction of MnSOD. This suggests that IκBβ may have a specific negative modulatory effect on the expression of this gene. IκBα knock down also curtailed the TNFα-mediated autoregulation of gene expression, while IκBβ knock down caused a 2-fold higher level of induction over mtDNA-depleted cells treated with TNFα. Although the possible negative modulatory role of IκBβ in MnSOD and TNFα gene expression was surprising, these results collectively show the distinctive physiological roles of the two inhibitory proteins being compared here.

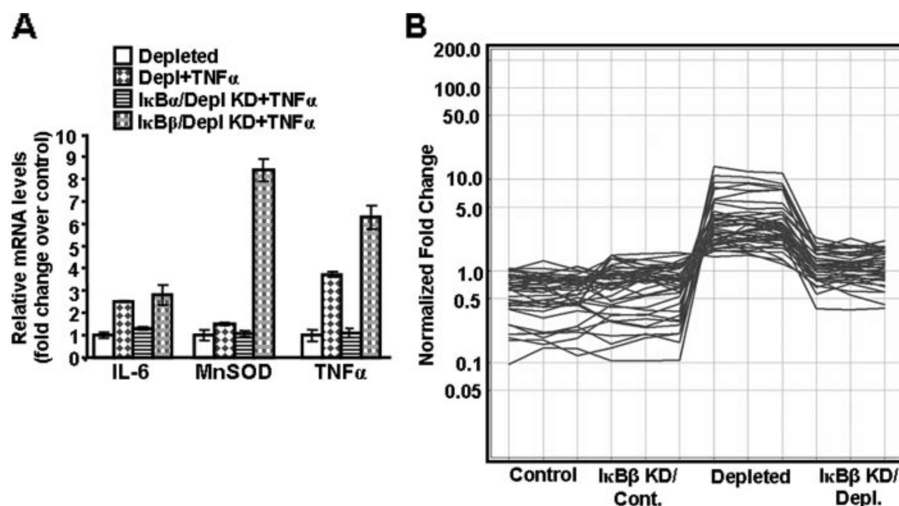

FIGURE 4. **Differential regulation of mitochondrial stress-responsive genes by IκBα and IκBβ proteins.** *A*, levels of induction of canonical NFκB-regulated genes IL-6, MnSOD, and TNFα by TNFα treatment (10 ng/ml for 30 min) in mtDNA-depleted (*Depleted*), IκBα knockdown/depleted (*IκBα KD/Depl*), or IκBβ knockdown/depleted (*IκBβ KD/Depl*) cells. mRNA levels were quantified by real-time PCR using total RNA as described under "Materials and Methods." The levels of β-actin were used for normalizing the values. The values are the average of reactions run in triplicates. *B*, cDNA microarray analysis was carried out on a Affymetrix mouse gene array using three independent samples of total RNA isolated from C2C12 control, IκBβ knockdown control (*IκBβ KD/Cont.*), mtDNA-depleted (*Depleted*), and IκBβ knockdown mtDNA-depleted (*IκBβ KD/Depl.*) cells. Analysis was carried out as described under "Materials and Methods."

We carried out cDNA microarray analysis to understand the range of genes affected by the mitochondrial stress-activated NFκB signaling and the involvement of IκBβ in the expression of these genes. Total RNA from control and depleted C2C12 cells with or without siRNA-based knock down of IκBβ was analyzed. We identified a set of genes that were up-regulated at least 2-fold by mtDNA depletion in a manner that was dependent upon the activity of IκBβ. As represented in Fig. 4*B* and Table 1, ~40 genes fit these criteria. For these genes the effect of mtDNA depletion was

TABLE 1

Genes regulated by IκBβ during mitochondrial respiratory stress signaling

Depl., depleted; *Cont.*, control.

Gene title	Gene symbol	-Fold change (depl. vs. cont.)	-Fold change (depl. vs. depl.IκBβ KD)
Tumor marker proteins			
Melanoma cell adhesion molecule	*Mcam*	26.1938	−2.12697
Melanoma antigen	*Mela*	14.4641	1.01304
Tumor progression proteins			
Breast cancer anti-estrogen resistance 1	*Bcar1*	2.47854	1.12202
Transforming growth factor, β2	*Tgfb2*	2.2924	−1.50422
Metabolism regulatory proteins			
Carbonic anhydrase 8	*Car8*	22.0069	1.15188
Insulin-like growth factor 2, binding protein 1	*Igf2bp1*	10.4676	−1.40136
Pyruvate dehydrogenase kinase, isoenzyme 1	*Pdk1*	4.12998	−1.52081
Pyruvate carboxylase	*Pcx*	3.2003	1.04495
Phosphofructokinase, platelet	*Pfkp*	3.1962	−1.65984
Pyruvate dehydrogenase kinase, isoenzyme 3	*Pdk3*	2.50058	−1.45416
Cytoskeletal proteins			
Procollagen, type IV, α1	*Col4a1*	6.88394	−1.07038
Procollagen, type IV, α2	*Col4a2*	6.23115	1.0008
Connective tissue growth factor	*Ctgf*	5.01523	−1.53219
Cell/mitochondrial function/signaling proteins			
Cytochrome *c* oxidase, subunit VIIa 1	*Cox7a1*	5.82145	−1.89848
Nitric-oxide synthase 1, neuronal (Nos1), mRNA	*Nos1*	8.47653	−1.24509
Synuclein, α	*Snca*	9.44693	−2.23639
Ubiquitin-activating enzyme E1-like	*Ube1l*	7.93742	−1.3696
Mitogen-activated protein kinase kinase kinase 1	*Map3k1*	4.30808	−1.76614
Glycogen synthase 1, muscle/glycogen synthase 3, brain	*Gys1///Gys3*	3.21247	−1.39839
Superoxide dismutase 2, mitochondrial	*Sod2*	2.47852	−1.19618
Translocase of inner mitochondrial membrane 9 homolog (yeast)	*Timm9*	2.37736	−1.51778
Phosphatidylinositol 3-kinase, C2 domain-containing, α polypeptide	*Pik3c2a*	2.3394	−1.56545
Calcium regulation proteins			
Inositol 1,3,4-triphosphate 5/6 kinase	*Itpk1*	3.88386	−1.25792
Calcium channel, voltage-dependent, P/Q type, α 1A subunit	*Cacna1a*	2.73045	−2.07777
FK506-binding protein 5	*Fkbp5*	1.89555	−1.40141

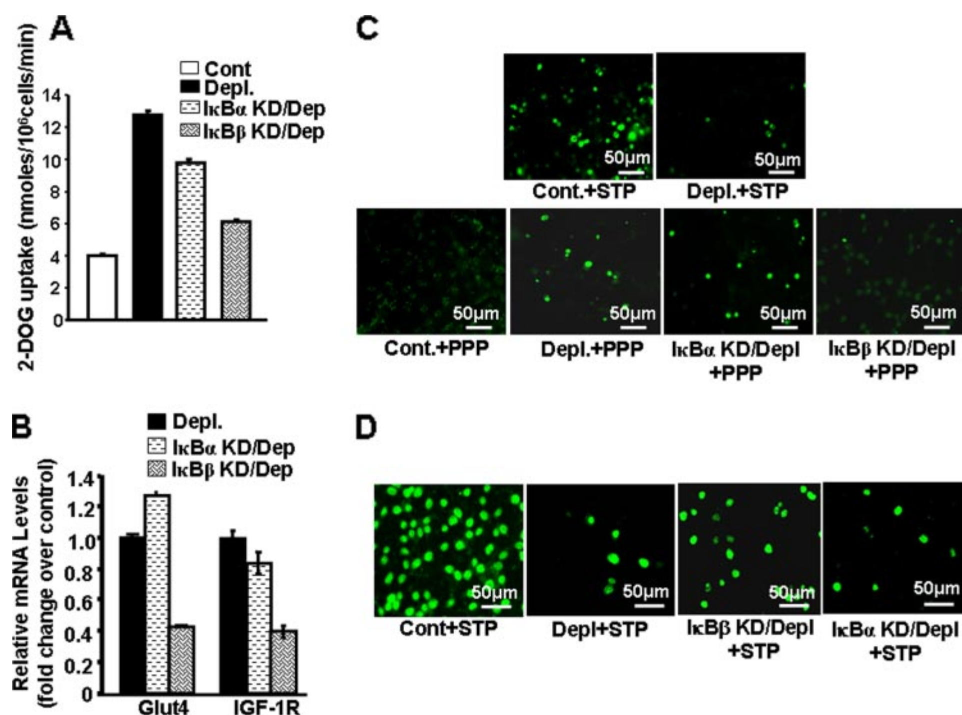

FIGURE 5. **Role of IκBβ-initiated NFκB in the regulation of mitochondrial respiratory stress-induced metabolic shift and cell death response.** *A*, uptake of [^{3}H]2-deoxyglucose (*DOG*) was measured in control C2C12 (*Cont*), mtDNA-depleted (*Depl.*) and IκBα KD and IκBβ KD cells. Cells (1×10^6) were grown in 6-well plates and incubated with [^{3}H]2-deoxyglucose, and the glucose uptake was measured in terms of radioactive counts incorporated in the cells as detailed under "Materials and Methods." *B*, levels of mitochondrial respiratory stress-mediated expression of Glut4 and IGF-1R genes were measured in IκBα and IκBβ mRNA knockdown cells by real-time PCR as described under "Materials and Methods." β-actin was used as internal control for normalizing the values. Values are the average of readings obtained from three separate reactions in both *A* and *B*. *C*, the role of IκBβ-initiated NFκB pathway in stress-induced glucose metabolism and cell death response was assessed using the IGF-1R-specific inhibitor picropodophyllin (*PPP*) (2.5 μM) in the indicated cell lines. Cell death was detected by fluorescent terminal deoxynucleotidyltransferase-mediated dUTP nick end-labeling (TUNEL) assay as described before (15) using Apop Tag kit from Intergen Co. STP-mediated cell death in control (*Cont.*) and mtDNA-depleted (*Depl.*) cells was used as positive control for apoptotic cell death. *D*, apoptotic cell death in response to staurosporine (*STP*) was assessed in the indicated cell lines. Cells grown on coverslips were treated with 2 μM STP for 4 h, and the apoptotic cells were detected by TUNEL assay as described above.

mediated by signaling through IκBβ. Importantly, there was no significant change in the level of expression of these genes in control cells with IκBβ knock down. The up-regulated genes represent diverse roles in cellular metabolism, including regulating signal transduction, cellular redox function, ion transport, glucose metabolism, mitochondrial energetics, cell adhesion, cell cycle, and tumorigenesis (see Table 1). These results show that IκBβ plays a critical role in the mitochondrial stress-induced NFκB activation and that this pathway affects the expression of a large number of nuclear genes associated with an array of critical cellular functions.

The NFκB-dependent Mitochondrial Stress Response Pathway Modulates Glucose Uptake and Regulates the Expression of Glut4 and IGF-1R—A characteristic feature of fast growing tumor cells is high utilization of glucose in glycolysis despite adequate oxygen utilization and mitochondrial electron transport function (33, 34, 37). Energy thus derived supports uninhibited tumor cell proliferation. Previously we and others have shown that the mtDNA-depleted cells have altered metabolism and invasive properties (16, 31, 33, 38–40). Therefore, we examined the glucose uptake capability of the mtDNA-depleted cells and investigated whether IκBβ mRNA knock down affects glucose uptake. In keeping with our recent results, mtDNA-depleted cells showed significantly elevated levels of glucose uptake as compared with controls (Fig. 5*A*). IκBβ mRNA knock down blocked 60% of this increase. IκBα mRNA knock down also reduced glucose uptake, although to a lesser extent.

In a recent study we showed that mtDNA depletion or treatment with mitochondrial ionophores like CCCP induced the IGF-1R-regulated pathway (31). Real-time PCR results in Fig. 4*B* show that the increase in Glut4 and IGF-1R mRNA in response to mitochondrial stress was markedly abated by IκBβ mRNA knock down, suggesting that mitochondrial stress-mediated metabolic shift requires functional IκBβ-dependent NFκB pathway. Notably, IκBα knock down caused a further increase in Glut4 mRNA levels, suggesting its negative modulatory role on gene expression. In the case of IGF-1R mRNA, the effect of IκBα knock down was comparatively marginal compared with the effect of IκBβ mRNA knock down (Fig. 5*B*). Further, we tested the effect of picropodophyllin, a specific inhibitor of the IGF-1 receptor (41) that induces apoptosis in mtDNA-depleted cells (31). The terminal deoxynucleotidyltransferase-mediated dUTP nick end-labeling (TUNEL) assay results in Fig. 5*C* show that the depleted as well as IκBα KD/Depl cells had vastly increased number of apoptotic cells in response to picropodophyllin addition but IκBβ mRNA knock down had no effect on picropodophyllin susceptibility, similar to the control cells (Fig. 5*C*). These results confirm the importance of IκBβ in the regulation of nuclear gene expression and metabolic function of cells undergoing mitochondrial genetic stress.

IκBβ-dependent NFκB Activation Plays a Role in Mitochondrial Stress-induced Survival and Invasiveness—C2C12 skeletal muscle cells and A549 lung carcinoma cells subjected to mitochondrial stress developed increased invasiveness and resistance to staurosporine- (STP) and etoposide-mediated apoptosis (15, 27, 30). In this study we tested the role of IκBβ-dependent signaling in stress-induced resistance to apoptosis. Depleted cells showed markedly reduced STP-induced apoptosis compared with control cells but IκBβ knock down in these cells impeded resistance to apoptosis (Fig. 5*D*). IκBα knock down, on the other hand, did not change the number of cells undergoing apoptosis. These results suggest that IκBβ-dependent signaling is important

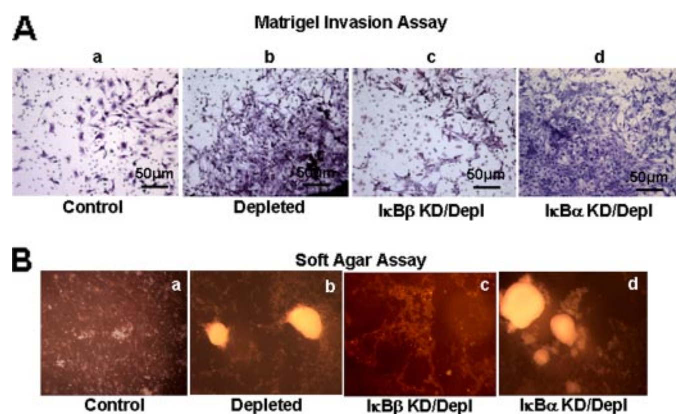

FIGURE 6. **Reversal of respiratory stress-mediated invasive property and cell proliferation by IκBβ mRNA silencing.** *A*, migration of cells across Matrigel matrix membrane was assayed in control (*a*), mtDNA-depleted (*Depleted*) (*b*), IκBα KD/Depl (*c*), and IκBβ KD/Depl (*d*). Invasion chambers were coated with Matrigel diluted 1:3 with serum-free Dulbecco's modified Eagle's medium, and 4×10^4 cells were seeded on Matrigel layer. Matrigel containing the noninvaded cells was removed from each well, and the invaded cells across the porous membrane were stained with hematoxylin. The stained cells were visualized under bright field microscope as described under "Materials and Methods." *B*, the role of IκBβ in supporting the invasive property of mtDNA-depleted cells was investigated by adherence-independent growth of control (*a*), depleted (*b*), and depleted cells knocked down for IκBβ expression (*IκBβ KD/Depl*) (*c*). Effect of IκBβ knock down on cell growth was compared with that of IκBα KD/Depl cells (*d*). 2×10^3 cells were grown in 6-well plates containing layers of 2% agar. Adherence-independent growth was assessed as described under "Materials and Methods."

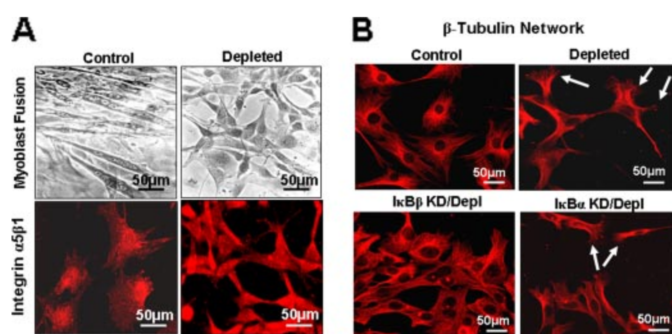

FIGURE 7. **Effect of IκBβ knock down on respiratory stress-mediated changes in cell morphology and cytoskeletal organization.** *A*, fusion of myoblasts into multinucleated myotube structure was determined by serum deprivation in control and mtDNA-depleted cells (*upper panels*). Cells were grown on coverslips in regular (10% fetal bovine serum) growth medium and after 48 h replaced with differentiating Dulbecco's modified Eagle's medium containing 2% fetal bovine serum. Cells were grown for another 48 h, and the phase contrast images were captured using an Olympus BX61 microscope. The control cells showed formation of multinucleated myotubes whereas they were absent in depleted cells. The cells were also immunostained for integrin α5β1 (*lower panels*) as described under "Materials and Methods," and images were taken using a fluorescence microscope. *B*, changes in cytoskeletal organization were detected by immunostaining of control, depleted, IκBβ KD/Depl, and IκBα KD/Depl cells with β-tubulin antibody as described under "Materials and Methods." *Arrows* indicate the filopodia with newly formed tubulin network.

in mediating mitochondrial stress-induced resistance to apoptosis.

We used the Matrigel invasion assay to show that that mtDNA depletion causes a marked increase in invading cells (Fig. 6*A*). IκBβ knock down, but not IκBα knock down, reversed the level of invasion to near control cell level, confirming the role of the IκBβ-dependent NFκB pathway in the propagation of mitochondrial stress signaling. It is also apparent from the growth pattern in soft agar (Fig. 6*B*) that mtDNA-depleted cells proliferated into an attachment-independent mass of cells while control and IκBβ knock down cells grew as monolayers on soft agar (Fig. 6*B*).

The Role of IκBβ in Mitochondrial Stress-induced Changes in Cytoskeletal Structure and Function—C2C12 cells differentiate to form multinucleated myotubes in response to serum deprivation. MtDNA depletion markedly affected the ability of cells to form multinucleated myotubes (Fig. 7*A*). Consistent with the altered myogenic property, mtDNA-depleted cells contained markedly reduced levels of α5β1 integrins around the plasma membrane. In view of the suggested role of integrins in skeletal myogenesis (42), our results suggest that mitochondrial stress signaling disrupts myogenesis.

To further investigate the nature of cytoskeletal changes in response to mitochondrial stress, we examined the tubulin network in mtDNA-depleted cells. MtDNA-depleted cells have an abnormal cytoskeletal organization with extensively condensed tubulin organization (Fig. 7*B*). Tubulin bundles were concentrated around the filopodia-like structures. IκBβ (but not IκBα) mRNA knock down reverted the cytoskeletal disorganization, providing a possible mechanistic explanation for the reduction of invasiveness seen previously.

DISCUSSION

Role of IκBβ in Mediating Mitochondrial Stress Signaling—In this study we have provided evidence for the intermediaries of the NFκB pathway that propagate mitochondria-to-nucleus stress signaling and stress-mediated changes in cell morphology and phenotype. Specifically, our results show that IκBβ is a key regulatory molecule in modulating mitochondrial stress signaling and activating a set of genes that are distinct from classical NFκB targets. The dependence on Cn for the activation of NFκB in mitochondrial stress signaling is unique and appears to be specific to this signaling pathway (28). The results also point to the possibility that the IκBβ-dependent pathway plays an important role in the activation of tumor-promoting genes through NFκB/cRel, thus presenting an additional and specific molecular target for controlling oncogenic progression. In this study we have also demonstrated the importance of IκBβ in the mitochondrial stress-mediated metabolic switch and cytoskeletal reorganization.

A number of studies have implicated NFκB signaling in tumor development and progression (43, 44). Studies have also suggested that NFκB-dependent tumorigenesis and invasion are cell- and tissue-specific (44–46). Many of these studies point to the possibility that NFκBs activate anti-apoptotic genes, providing protection against cell death and thus supporting the proliferation of tumor cells (47–49). Constitutive expression of NFκB in tumors has been suggested to play critical roles in tumor cell chemoresistance, growth promotion, invasion, metastasis, and tumor angiogenesis (50–53). Attempts to develop pharmacological interventions based upon NFκB blockade for the treatment of cancer have been largely unsuccessful because of the side effects of NFκB inhibition (4). Furthermore, the small molecule inhibitors of IKK or NFκB that have been developed have not been sufficiently specific (50).

Distinctive Features of IκBβ-mediated NFκB Pathway—There is increasing evidence that the interaction of Rel proteins with IκB inhibitory proteins is a necessary regulatory step for activation of the NFκB pathway (54–56). Absence of these inhibitory proteins severely affects the nuclear translocation of NFκB/Rel transcription factors to the nucleus and activation of NFκB-responsive genes. Consistent with this view, we have shown that the IκBβ-dependent pathway plays a critical role in the mitochondrial respiratory stress-mediated resistance to apoptosis and in tumor cell invasion.

Because of its slow turnover rate and relatively unchanging steady state levels in response to cytokine and chemokine treatment, IκBβ is believed to regulate the constitutive NFκB pathway while IκBα is involved in the inducible phase of regulation (57, 58). In cells treated with TNFα or interleukins, IκBα is transcriptionally induced within minutes of treatment and undergoes rapid turnover at the end of signaling (59–61). The level of IκBβ, on the other hand, undergoes only a marginal change in response to these inducers (27, 57, 62). Detailed biochemical and crystal structure studies suggest that binding and affinity of IκBα to p65 homodimers significantly differ from that of IκBβ. IκBβ binds to Rel factors more tightly, masking their nuclear translocation signal and preventing nuclear entry of oligomeric complexes (60). Chemical cross-linking of cytosolic fractions from mtDNA-depleted cells suggested that IκBβ largely exists in a complex with c-Rel and p50 heterodimers (28).

The results of this study confirm the functional distinction between IκBβ and IκBα in mitochondrial stress signaling. In our experiments, the knock down of IκBβ, but not IκBα, decreased the nuclear localization of p50 and cRel as well as the expression of target gene RyR1 and Cath L. IκBβ knock down also blocked the changes in morphology, viability, and glucose uptake found in mtDNA-depleted cells. Additionally, knock down of IκBβ reversed many of the changes in nuclear gene expression induced by mtDNA depletion seen in transcriptional arrays, implicating this protein in mitochondria-to-nucleus communication. Remarkably, IκBβ knock down also enhanced the TNFα-mediated increase in downstream mRNA expression, in marked contrast to the effect of IκBα knock down. These results provide compelling evidence for different physiological roles for the two major IκB proteins, although there may be some overlap in the nuclear targets of these factors as observed in the expression of Glut4 and IGF-1R.

Permissive Role of IκBβ as Opposed to Inhibitory Role of IκBα—Many studies have shown that IκBα degradation following cytokine or chemokine induction triggers a marked increase in the nuclear localization of p65:p50 Rel proteins and induced expression of target genes. IκBα knock down in mtDNA-depleted cells also resulted in the increased nuclear localization of p65:p50 in keeping with its well acknowledged "inhibitory" function. In contrast, knock down of IκBβ mRNA caused a marked reduction in the nuclear cRel:p50 levels, suggesting that IκBβ does not function as a classical inhibitor. In fact, cytosolic IκBβ and Cn are required for the release of active cRel:p50 and their nuclear translocation (28). Therefore, IκBβ is more accurately described as having a permissive role in NFκB signaling in response to mitochondrial stress. In summary, we present compelling evidence for the distinct physiological roles of IκBβ and IκBα in mediating the NFκB signaling. The calcineurin-regulated activation of IκBβ in response to mitochondrial stress is an important landmark of this extensive signaling pathway that is interrupted by blocking the IκBβ mRNA expression. As outlined in the model presented in Fig. 8, IκBβ knock down inhibits the various morphologic and functional changes seen in response to mitochondrial stress.

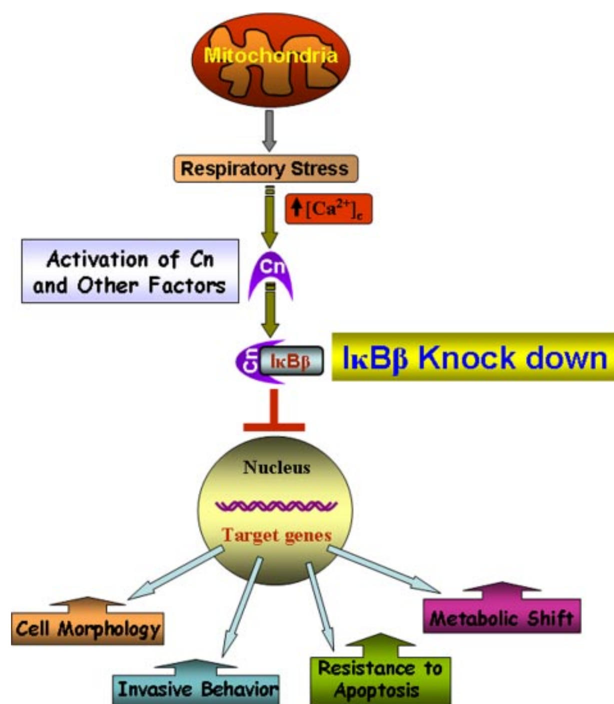

FIGURE 8. **IκBβ as a critical landmark factor in respiratory stress signaling pathway.** A model showing interruption of mitochondrial stress signaling that regulates different aspects of cellular processes in IκBβ mRNA-silenced cells.

Acknowledgments—We thank Dr. Michael May, School of Veterinary Medicine, University of Pennsylvania, for providing the real-time PCR primers for IL-6, MnSOD, and TNFα. We also thank members of the Avadhani laboratory for useful suggestions and comments.

REFERENCES

1. Perkins, N. D., and Gilmore T. D. (2006) *Cell Death Differ.* **13,** 759–772
2. Ghosh, S., and Karin, M. (2002) *Cell* **109,** (Suppl.) S81–S96
3. Hayden, M. S., and Ghosh, S. (2004) *Genes Dev.* **18,** 2195–2224
4. Gilmore, T. D., Cormier, C., Jean-Jacques, J., and Gapuzan, M. E. (2001) *Oncogene* **20,** 7098–7103
5. Luo, J. L., Kamata, H., and Karin, M. (2005) *J. Clin. Investig.* **115,** 2625–2632
6. Karin, M. (2006) *Nature* **441,** 431–436
7. Perkins, N. D. (1997) *Int. J. Biochem. Cell Biol.* **29,** 1433–1448
8. Saccani, S., Pantano, S., and Natoli, G. (2003) *Mol. Cell* **11,** 1563–1574
9. Kato, T., Jr., Delhase, M., Hoffmann, A., and Karin, M. (2003) *Mol. Cell* **12,** 829–839
10. Romieu-Mourez, R., Landesman-Bollag, E., Seldin, D. C., and Sonenshein, G. E. (2002) *Cancer Res.* **62,** 6770–6778
11. Tergaonkar, V., Bottero, V., Ikawa, M., Li, Q., and Verma, I. M. (2003) *Mol. Cell. Biol.* **23,** 8070–8083
12. Imbert, V., Rupec, R. A., Livolsi, A., Pahl, H. L., Traenckner, E. B., Mueller-Dieckmann, C., Farahifar, D., Rossi, B., Auberger, P., Baeuerle, P. A., and

Peyron, J. F. (1996) *Cell* **86,** 787–798
13. Schoonbroodt, S., Ferreira, V., Best-Belpomme, M., Boelaert, J. R., Legrand-Poels, S., Korner, M., and Piette, J. (2000) *J. Immunol.* **164,** 4292–4300
14. Biswas, G., Adebanjo, O. A., Freedman, B. D., Anandatheerthavarada, H. K., Vijayasarathy, C., Zaidi, M., Kotlikoff, M., and Avadhani, N. G. (1999) *EMBO J.* **18,** 522–533
15. Biswas, G., Anandatheerthavarada, H. K., and Avadhani, N. G. (2005a) *Cell Death. Differ.* **12,** 266–278
16. Amuthan, G., Biswas, G., Ananadatheerthavarada, H. K., Vijayasarathy, C., Shephard, H. M., and Avadhani, N. G. (2002) *Oncogene* **21,** 7839–7849
17. Arnould, T., Vankoningsloo, S., Renard, P., Houbion, A., Ninane, N., Demazy, C., Remacle, J., and Raes, M. (2002) *EMBO J.* **21,** 53–63
18. Dey, R., and Moraes, C. T. (2000) *J. Biol. Chem.* **275,** 7087–7094
19. Kim, J. Y., Kim, Y. H., Chang, I., Kim, S., Pak, Y. K., Oh, B. H., Yagita, H., Jung, Y. K., Oh, Y. J., and Lee, M. S. (2002) *Oncogene* **21,** 3139–3148
20. Petros, J. A., Baumann, A. K., Ruiz-Pesini, E., Amin, M. B., Sun, C. Q., Hall, J., Lim, S., Issa, M. M., Flanders, W. D., Hosseini, S. H., Marshall, F. F., and Wallace, D. C. (2005) *Proc. Natl. Acad. Sci. U. S. A.* **102,** 719–724
21. Shirada, Y., Yamagata, K., Kanamori, T., Nakano, K., Kwong, J. Q., Manfredi, G., Oda, H., and Ohta, S. (2005) *Cancer Res.* **65,** 1655–1663
22. Biswas, G., Srinivasan, S., Anandatheerthavarada, H. K., and Avadhani N. G. (2008) *Proc. Natl. Acad. Sci. U. S. A.* **105,** 186–191
23. Srinivasan, S., and Avadhani, N. G. (2007) *Ann. N. Y. Acad. Sci.* **1117,** 51–61
24. Epstein, C. B., Waddle, J. A., Hale, V. W., Davé, V., Thornton, J., Macatee, T. L., Garner, H. R., and Butow, H. R. (2001) *Mol. Biol. Cell* **12,** 297–308
25. Sekito, T., Liu., Z., Thornton., J., and Butow, R. A. (2002) *Mol. Biol. Cell* **13,** 795–804
26. Passos, J. F., von Zglinicki, T., and Kirkwood, T. B. (2007) *BioEssays* **29,** 908–917
27. Amuthan, G., Biswas, G., Zhang, S. Y., Klein-Szanto, A., Vijayasarathy, C., and Avadhani, N. G. (2001) *EMBO J.* **20,** 1910–1920
28. Biswas G., Anandatheerthavarada, H. K., Zaidi, M., and Avadhani, N. G. (2003) *J. Cell Biol.* **161,** 507–519
29. Butow, R. A., and Avadhani, N. G. (2004) *Mol. Cell* **14,** 1–15
30. Biswas, G., Guha, M., and Avadhani, N. G. (2005) *Gene* **354,** 132–139
31. Guha, M., Srinivasan, S., Biswas, G., and Avadhani, N. G. (2007) *J. Biol. Chem.* **282,** 14536–14546
32. Kang, B. P., Urbonas, A., Baddoo, A., Baskin, S., Malhotra, A., and Meggs, L. G. (2003) *Am. J. Physiol.* **285,** F1013–F1024
33. Pelicano, H., Xu, R.-X., Du, M., Feng, L., Sasaki, R., Carew, J. S., Hu, Y., Ramdas, L., Hu, L., Keating, M. J., Zhang, W., Plunkett, W., and Huang, P. (2006) *J. Cell Biol.* **175,** 913–923
34. Girnita, A., All-Ericsson, C., Economou, M. A., Astrom, K., Axelson, M., Seregard, S., Larsson, O., and Girnita, L. (2006) *Clin. Cancer Res.* **12,** 1383–1391
35. Szalai, G., Krishnamurthy, R., and Hajnóczky, G. (1999) *EMBO J.* **18,** 6349–6361
36. Frevert, E. U., and Kahn, B. B. (1997) *Mol. Cell. Biol.* **17,** 190–198
37. Warburg, O. (1956) *Science* **123,** 309–314
38. Modica-Napolitano, J. S., Kulawiec, M., and Singh, K. K. (2007) *Curr. Mol. Med.* **7,** 121–131
39. Coloff, J. L., and Rathmell, J. C. (2006) *J. Cell Biol.* **175,** 845–847
40. van Waveren, C., Sun, Y. B., Cheung, H. S., and Moraes, C. T. (2006) *Carcinogenesis* **27,** 409–418
41. Stromberg, T., Ekman, S., Girnita, L., Dimberg, L. Y., Larsson, O., Axelson, M., Lennartsson, J., Hellman, U., Carlson, K., Osterborg, A., Vanderkerken, K., Nilsson, K., and Jernberg-Wiklund, H. (2006) *Blood* **107,** 669–678
42. Boettiger, D., Enomoto-Iwamoto, M., Yoon, H. Y., Hofer, U., Menko, A. S., and Chiquet-Ehrismann, R. (1995) *Dev. Biol.* **169,** 261–272
43. Karin, M., Cao, Y., Greten, F. R., and Li, Z. W. (2002) *Nat. Rev. Cancer.* **2,** 301–310
44. Gilomre, T. D. (2003) *Cancer Treat. Res.* **115,** 241–265
45. Wang, C. Y., Cusack, J. C., Jr., Liu, R., and Baldwin, S., Jr. (1999) *Nat. Med.* **5,** 412–417
46. Lind, D. S., Hochwald, S. N., Malaty, J., Rekkas, S., Hebig, P., Mishra, G., Moldawer, L. L., Copeland, E. M., III, and Mackay, S. (2001) *Surgery* **130,** 363–369
47. Wang, C-Y., Mayo, M. W., and Baldwin, A. S., Jr. (1996) *Science* **274,** 784–787
48. Beg, A. A., and Baltimore, D. (1996) *Science* **274,** 782–784
49. Liu, Z-G., Hu, H., Goeddel, D. V., and Karin, M. (1996) *Cell* **87,** 565–576
50. Greten, F. R., and Karin, M. (2004) *Cancer Lett.* **206,** 193–199
51. Bargou, R. C., Emmerich, F., Krappmann, D., Bommert, K., Mapara, M. Y., Arnold, W., Royer, H. D., Grinstein, E., Greiner, A., Scheidereit, C., and Dörken, B. (1997) *J. Clin. Investig.* **100,** 2961–2969
52. Duffey, D. C., Chen, Z., Dong, G., Ondrey, F. G., Wolf, J. S., Brown, K., Siebenlist, U., and Van Waes, C. (1999) *Cancer Res.* **59,** 3468–3474
53. Huang, S., Pettaway, C. A., Uehara, H., Bucana, C. D., and Fidler, I. J. (2001) *Oncogene* **20,** 4188–4197
54. Tergaonkar, V., Correa, R. G., Ikawa, M., and Verma, I. M. (2005) *Nat. Cell Biol.* **7,** 921–923
55. Grilli, M., Chiu, J. S., and Lenardo, M. J. (1993) *Int. Rev. Cytol.* **143,** 1–62
56. May, M. J. (2006) *J. Immunol.* **177,** 7483–7484
57. Thompson, J. E., Phillips, R. J., Erdjument-Bromage, H., Tempst, P., and Ghosh, S. (1995) *Cell* **80,** 573–582
58. Thanos, D., and Maniatis, T. (1995) *Cell* **80,** 529–532
59. Miyamoto, S., Maki, M., Schmitt, M. J., Hatanaka, M., and Verma, I. M. (1994) *Proc. Natl. Acad. Sci. U. S. A.* **91,** 12740–12744
60. Malek, S., Chen, Y., Huxford, T., and Ghosh, G. (2001) *J. Biol. Chem.* **276,** 45225–45235
61. Scherer, D. C., Brockman, J. A., Chen, Z., Maniatis, T., and Ballard, D. W. (1995) *Proc. Natl. Acad. Sci. U. S. A.* **92,** 11259–11263
62. Miyamoto, S., Seufzer, B. J., and Shumway, S. D. (1998) *Mol. Cell. Biol.* **18,** 19–29